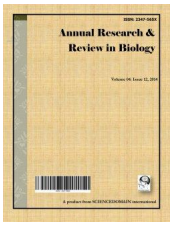

Annual Research & Review in Biology

20(2): 1-15, 2017; Article no.ARRB.36586
ISSN: 2347-565X, NLM ID: 101632869

Osteogenic Potential of Zirconium Enriched Bioglass on Differentiated Amniotic Fluid Derived Stem Cells and Healing of Tibia Rabbit Defect

Zeinab A. Salem[1], Eman E. A. Mohammed[2*], Khaled R. Gaber[3] and Hanan H. Beherei[4]

[1]Department of Oral Biology, Faculty of Oral and Dental Medicine, Cairo University, Egypt.
[2]Department of Medical Molecular Genetics, National Research Centre (NRC), Cairo, Egypt.
[3]Department of Prenatal Diagnosis and Fetal Medicine, National Research Center, Cairo, Egypt.
[4]Department of Ceramics, Biomaterials Group, National Research Center, El- Bohouth Street, 12622 Cairo, Egypt.

Authors' contributions

This work was carried out in collaboration between all authors designed the study. Author ZAS designed the study, manage the in-vivo study, application and histopathology, performed the statistical analysis, wrote the protocol and wrote the first draft of the manuscript. Author EEAM managed the in-vitro study of isolation, culture, characterization of Amniotic fluid sample. Author KRG provided us with the amniotic fluid sample. Author HHB managed preparation and characterization of novel nano-bioactive glass including zirconium (NZBG). All authors read and approved the final manuscript.

Article Information

DOI: 10.9734/ARRB/2017/36586
Editor(s):
(1) Sujan Banik, Assistant Professor, Department of Pharmacy, Noakhali Science and Technology University, Bangladesh.
(2) George Perry, Dean and Professor of Biology, University of Texas at San Antonio, USA.
Reviewers:
(1) Jonathan Lowery, Marian University College of Osteopathic Medicine, USA.
(2) Wagih mommtaz ghannam, Mansoura university, Egypt.
(3) Saif khan, Dr. Z. A. Dental College, Aligarh Muslim University, India.
Complete Peer review History: http://www.sciencedomain.org/review-history/21998

Original Research Article

Received 1st September 2017
Accepted 14th November 2017
Published 21st November 2017

ABSTRACT

Aims: The regeneration prospects of human bone seem to be confined due to different systemic and environmental conditions that may affect many patients. This work aimed to evaluate the biocompatibility and osteogenic potential of the prepared novel nano-bioactive glass including zirconium (NZBG) in-vitro and in-vivo studies.

**Corresponding author: E-mail: Em_mohammed00@yahoo.com;*
E-mail: zeinab.salem@dentistry.cu.edu.eg;

Study Design: The novel nano-bioactive glass (NZBG) was fabricated by sol- gel rout for the development of bone tissue replacement.
Place and Duration of Study: NZBG: Faculty of Oral and Dental Medicine Dept. (Cairo University), Medical molecular genetics Dept. (National Research Centre (NRC), Prenatal diagnosis and fetal medicine Dept. (National Research Center) and Ceramics Dept., Biomaterials group (National Research Center) between June 2015 and July 2017.
Methodology: The novel nano-bioactive glass (NZBG) was fabricated by sol- gel rout for the development of bone tissue replacement. The prepared nano-bioactive glass (NZBG) was characterized by Photo correlation spectroscopy (PCS), transmission electron microscope (TEM), X-ray powder diffraction (XRD) and Fourier Transform infrared spectroscopy (FTIR) before the in-vitro and in-vivo studies. The in-vitro evaluation of nano-bioactive glass NZBG was obtained through seeding human osteogenic cells from amniotic fluid derived stem cells on NZBG disks in culture for different time periods, 7 and 21days. The cultures were examined for mineralization by Alizarin Red Staining. The in-vitro mineralization was evaluated by scanning electron microscopy- X-ray microanalysis (SEM- EDAX) test.
The in-vivo evaluation was done on thirty adult rabbits weighing between 2 kg and 2.5 kg. Two holes in each tibia, with a diameter of 2 mm were prepared. One of them was left without treatment as control group and the other was filled with NZBG bioactive glass. The animals were euthanized after 1, 2 and 3 weeks. The defects were examined histologically by H&E, histochemically by Masson's trichrome stain and histomorphometrically.
Results: The in-vitro examination showed the enhanced osteoblastic proliferation over the NZBG bioactive glass disks and clusters of bone like apatite mineralization in multilayer arrangements that increased by time. While the in-vivo study demonstrated well and proper healing of the defect filled with NZBG bioactive glass regarding the bone quality and quantity in comparison to the control group.
Conclusion: An enhanced biocompatibility and faster osteogenesis with the prepared NZBG bioactive glass. This is meaning the prediction good potential applications to bone regeneration medicine.

Keywords: Zirconium; nano bioactive glass; in-vitro; in-vivo; osteogenic potential; biocompatibility.

1. INTRODUCTION

The regeneration potential of human bone appears to be limited due to different systemic and environmental conditions that may affect the patients. The regeneration prospects of human bone seems to be confined due to different systemic and environmental conditions that may affect many patients. [1]. Tissue engineering was proven to be a promising biomedical strategy for bone reconstruction following bone loss due to trauma or surgery [2]. There is an urgent need to use new bone replacement materials in the case of multiple fractures of bones. Ordinary bone replacement surgeries of first generation classes consists of autogenic or allogenic bone grafting [3]. Problems such as limited sources of donor bone, graft rejection, high costs and the risk of disease transmission might occur. Consequently, alternative treatment modalities to promote bone regeneration have been carefully examined [4].

Applying synthetic materials for bone regeneration, classified as osteoconductors, are an alternative to existing limitations and difficulties in obtaining autografts, and to the possibility of disease transmission by allografts [5]. The problem was that all materials available at the time, e.g. polymers that were designed to be bioinert, triggered fibrous encapsulation after placement, rather than forming a stable interface or bond with tissues. Professor Hench decided to make a degradable glass type 45S which contains the Na_2O, CaO, SiO_2 and P_2O_5, high in calcium content of 24.5% [1]. This opened the area of biomedical materials, with many new materials and products being formed from variations on bioactive glasses [1] and also glass–ceramics [6] and bioceramics such as synthetic hydroxyapatite (HA) and other calcium phosphates [7].

In exposure with body fluids, bioactive materials create a specific biological reaction at their surface which allows a strong bonding to surrounding bone tissues. This feature is recognized as bioactivity. When place in exposure with tissues, bioactive glasses exhibit

biocompatibility and non-attendance of inflammatory response. They can be non-active or bioactive consisting on their chemical structure and their surface morphology characteristic behavior [6,8]. Studies have obtained that bioglasses bond with bone more rapidly than other bioactive ceramics, and in vitro studies denote that their osteogenic properties are due to their biodegeneration of]products stimulating osteoprogenitor cells at the genetic level. However, calcium phosphates such as tricalcium phosphate and synthetic hydroxyapatite are more excessively utilized in the bone replacements. Some of the purposes are commercial, but others are due to the scientific restriction of the Hench –Bioglass [9].

Amniotic fluid cells are normally cultured for prenatal diagnosis but being having characteristics similar to embryonic stem cells (ESCs) they can have huge therapeutic applications in the form of cellular therapy and tissue engineering. They have additional advantage of being very less antigenic in nature [10]. Human amniotic fluid stem cells (AF-MSCs) were cultured on bioactive glass scaffolds and evaluated for their ability to differentiate into osteoblastic cells in-vivo [11]. This work aimed to evaluate the biocompatibility and osteogenic potential of the prepared novel nano-bioactive glass including zirconium (NZBG) in vitro and in vivo studies.

2. MATERIALS AND METHODS

2.1 Preparation Method of Zirconium Enriched Bioactive Glass in Nano Scale (NZBG)

The composition of novel nano-bioactive glass is listed in Table 1. The synthesis for the 6.7 g of tetraethyl orthosilicate (TEOS), 0.94 g of calcium nitrate ($Ca(NO_3)_2$-4H2O), 0.46 g of zirconium oxynitrate $ZrO(NO_3)_2 \cdot 3H_2O$, 0.73 ml of triethyl phosphate (TEP) and HNO_3 of 2M, used as catalyst, in 31.5 mL of H2O were dissolved in 60 ml of ethanol, and stirred at room temperature for 1 day. Then it was transferred to a Petri dish and squeezed out the excess solution after evaporating the solution for 12 h at room temperature. When the sample was completely dry, it was calcined at 700°C (ramp of 2°C/min) for 8 h to obtain the final Zr-incorporated bioactive glass with some modifications of method proposed by Montazerian et al. 2015.

2.2 Characterization of the Nzbg Powder

2.2.1 Photo correlation spectroscopy (PCS) & transmission electron microscopy (TEM)

Mean particle size diameter and poly disparity index of the prepared nano particles were measured directly after synthesis, using photo correlation spectroscopy (PCS) (Malvern Instruments Ltd, Worcestershire, UK). Briefly, a volume of 2 ml of the NZBG suspension were added to the quartz cell of the PCS and measurements were taken at 90° to the incident light source. Three separate measurements were made and their average was taken as the final reading. Transmission electron microscope (TEM) imaging of the NZBG particles to calculate its average size (TEM, Zeiss type EM10).

2.2.2 X-ray diffraction (XRD) analysis

To investigate the phase composition and crystallinity of the sample, x-ray diffraction (XRD) analysis was performed. Functional nature of the samples was obtained in a Diano X-ray diffractometer using Cu Kα radiation (λ = 0.1542 Å) produced applying a tube voltage of 40kV and a tube current of 40 mA [12].

2.2.3 Fourier transform infrared spectroscopy (FT-IR) analysis

The prepared sample was subjected x-ray diffraction (XRD) analysis to determine the stoichiometry deviations. FTIR was employed running in absorption mode, via potassium bromide (KBr) technique [0.2 mg of the sample was mixed with KBr powder (Sigma-Aldrich, FT-IR grade, P 99%), ground and then pressed by applying a pressure of 10 t in order to obtain a 1(mm) pellet, using a single beam computerized FT-IR (NEXAS 670, Nicolet, USA) in the frequency range of 4000-400 cm-1 at a scanning speed of 2 mm/sec. FT-IR was used to verify the XRD findings and to provide evidence of ionic substitution [12].

2.3 Cell Culture and Seeding of AF-MSCs

2.3.1 Isolation and culture of amniotic fluid sample

A second trimester Amniotic fluid sample was obtained by amniocentesis from 26 years old woman performed 16 weeks of gestation [13] at

Table 1. The mol ratio of the oxide composition of zirconium enriched bioactive glass

Bioactive galss composition	CaO	P2O5	SiO2	ZrO2
NZBG	5	5	80	10

National Research Center, Cairo, Egypt. Amniotic fluid sample was isolated by centrifugation and pelleting of cells [14]. High glucose Dubelco Modified Eagle Media (DMEM) (lonza, Belgium) were used for culture and expansion, supplemented with 10% fetal bovine serum (FBS) (lonza, Belgium), 2 mM glutamax (Gibco, Invitrogen, Life Technologies, USA), 100 units/ml penicillin and 100 Mg/ml streptomycin (Pen-Strep, Lonza, Belgium), 1X non-essential amino acids (NEAA) (Lonza, Belgium) and (3ng/ml) basic fibroblast growth factor (bFGF) (Sigma-Aldrich,USA) (Kunisaki et al. 2007). The cells were incubated in a humid 5% CO_2 atmosphere at 37°C in a CO2 incubator (Innova Co-170, New Brunswick Scientific, Scotland).

2.3.2 Differentiation of AF-MSCs into bone forming cells

AF-MSCs at passage three were used for osteogenic differentiation when reached 70% confluency by culturing in DMEM containing 20% FBS, 100 µg/ml penicillin & streptomycin and 1% glutamax, L-ascorbic acid 2-phosphate, β-glycerol phosphate and dexamethasone [15]. Inverted microscopy was used at passage 1 and 2 to follow the progress of the cells.

2.3.3 Alizarin red mineralization assay

Characterization of AF-MSCs osteogenic differentiation was assessed by Alizarin Red staining (pH 4.2) after 14 and 21 days in osteogenic differentiation medium. Briefly, AF-MSCs cultures were rinsed with PBS, followed by fixation in 4% formalin (in PBS) for 10 min and washed with distilled water before staining with Alizarin Red solution for 1 min. Nonspecific staining was removed by thoroughly washing in distilled water over 24 h. [16,17].

2.3.4 Seeding of osteogenic stem cells on nano-bioactive glass disks

In vitro osteogenic differentiation of AF-MSCs on NZBG disks of 10 mm diameters and 3 mm heights was carried out. NZBG disks were used as a carrier for cells and were placed in 6-well culture plates. The disks were washed 3 times with 70 % ethanol, exposure to U.V for an hour and then washed twice with osteogenic medium (1 hour for each rinse). AF-MSCs were seeded on nano- glass disks at density of 10x106and incubate at 37°C and osteogenic differentiation medium, DMEM containing 20% FBS, 100 µg/ml penicillin & streptomycin and 1% glutamax, L-ascorbic acid 2-phosphate, β-glycerol phosphate and dexamethasone [15] for one, two and three week respectively. Discs were fixed on day 7 and 21 using Glutaraldehyde [18].

2.3.5 Scanning Electron microscopy (SEM)of osteogenic stem cells on nano-glass disks

For SEM analysis, specimens cells were fixed in 2% gluteraldehyde in 0.1 M cacodylate buffer (pH 7.4). To preserve the lipid structures, specimens were gently washed in 0.2 M cacodylate buffer (pH 7.4) with the addition of 0.15 M saccharose for three changes every 20 minutes, post-fixed in 1% osmium tetroxide at room temperature for 1 hours, then given two quick changes of the previous buffer and gradually dehydrated in increasing ethanol concentrations (from 25 to 100%, 15% steps). Samples were then carried through critical point drying (CPD) according to standard procedure using liquid carbon dioxide, observed with a Philips XL20 Scanning Electron Microscope (SEM Philips XL 20; FEI, Eindhoven, The Netherlands) at 20 KV, high vacuum mode. Images were stored in TIF format with 1024 × 768 Grid of Pixels [13].

2.4 *In vivo* NZBG Discs Implantation

Thirty adult New Zealand white rabbits weighing 2-2.6 kg, with an average age of 4 months, were used in this study. The experimental protocol was reviewed and approved by the Ethics Committee of the Faculty of Oral and Dental Medicine, Cairo University. Material was sterilized by autoclave prior to surgical implantation. Rabbits were anesthetized by intramuscular injection of a mixture of ketamine hydrochloride (50 mg/kg of body weight) and xylazine (5 mg/kg of body weight). The material was implanted in the lateral aspects of both left and right tibias of each rabbit. The implantation sit es were shaved, cleaned with antiseptic solution and incised then the

subcutaneous tissues and muscles were retracted to expose the bone. Four circular bony defects were produced in each animal, two in each tibia, using a diamond rounded surgical bure revolving at a low speed (25000 rpm) with copious physiological saline irrigation. Each defect was 2 mm in diameter and its depth extended down to the bone marrow (Fig. 1a). Upper hole in the right and left tibias were left without treatment and the lower holes were immediately filled with NZBG discs (Fig. 1b). The muscles, subcutaneous t issues and skin were sutured, and the wounds were sprayed with an antifungal-antibacterial spray. Post surgically animals were received an intravenous injection of Cephotaxime (10 mg\ Kg) once daily for 3 days [19]. The animals were euthanized by intravenous overdose of sodium pentobarbital at periods of 7, 14 and 28 days after surgery and their tibias were dissected free of soft tissues. Animal grouping was done according to Table 2.

2.5 Histological examination

The tibias were fixed in 10% calcium for mol for 48 hours then washed and soaked for eight weeks in 10% ethylene diamine tetra-acetic acid (EDTA) for decalcification. After that, the decalcified tibias were rinsed in distilled water, dehydrated in ascending grades of alcohol then embedded in paraffin. Sections of 5 µm were obtained and subjected to haematoxylin and eosin (H&E) staining for routine histological examination and to Masson's trichom stain for determining the newly formed bone.

2.6 Histomorphometric Analysis

Histomorphometric analysis was carried out by one investigator and the slides were coded so that the investigator was blind to the test groups. The histomorphometric data were obtained using Leica Qwin 500 image analyzer computer system controlled by Leica Qwin 500 software (Leica Microsystems, UK). The image analyzer was first calibrated automatically to convert the measurement units (pixels) produced by the image analyzer program into actual micrometer units. The area and the area percentage of newly formed bone trabeculae were measured using an objective lens having a magnification of 20x. Ten fields were measured for each specimen. Using the color detector, newly formed bone areas were masked by a blue binary color. The bone area percentage (bone area %) was calculated in relation to a standard measuring frame having an area of 118476.6 µm2. [20].

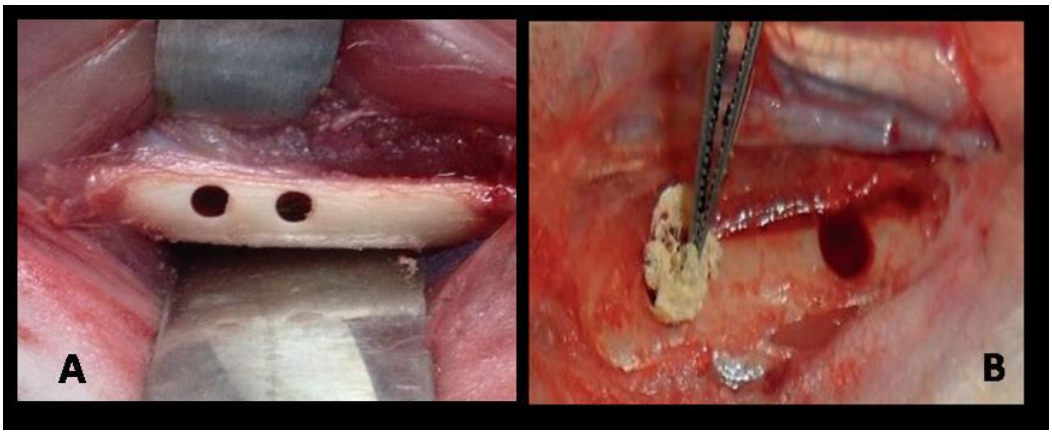

Fig. 1. The surgical procedure: (A): Two bony defects produced in one tibia, (B): The material being introduced into the bony defect

Table 2. Animal grouping

	Group A (left without NZBG)	Group B (NZBG)
Sacrificed at one week postoperative (PO)	Group A1	Group B1
Sacrificed at two weeks PO	Group A2	Group B2
Sacrificed at three weeks PO	Group A3	Group B3

2.6.1 Description of section

Tibia (long bone) cross section was used, bone diameter (B.Dm), the distance between external (Ex) and internal (In) periosteum, in the defect area was measured.

2.6.2 Area measurements

The area % of the newly formed bone /all bone area ratios were calculated in Masson trichrome stained sections (referent by having immature blue coloured collagen fibers in the Masson trichrome stained sections) using an objective lens having a magnification of 20x. Ten fields were measured for each specimen. Using the color detector, newly formed bone areas (with immature blue coloured collagen fibers) were masked by a green binary color. The bone area percentage (bone area %) was calculated in relation to a standard measuring frame having an area of 118476.6 µm2.

2.6.3 Units and dimensions

The histomorphometric data were obtained using Leica Qwin 500 image analyzer computer system controlled by Leica Qwin 500 software (Leica Microsystems, UK). The image analyzer was first calibrated automatically to convert the measurement units (pixels) produced by the image analyzer program into actual micrometer units.

2.7 Statistical Analysis

Post hoc test for independent samples was utilized when comparing two groups. A probability value less than 0.05 ($p < 0.05$) was considered statistically significant. All statistical calculations were done using the SPSS computer program (Statistical Package for the Social Science, SPSS Inc., Chicago, IL, USA) version 15 for Microsoft Windows.

3. RESULTS

3.1 PCS and Transmission Electron Microscopic Examination (TEM) of the Powder Morphology

PCS of NZBG particles showed that the average particle size was of 24±3 nm and a polydispersity index (PDI) of 0.015. The morphology of the nano particles was studied using transmission electron microscope indicated that the product is composed of nanostructures. The diameter is 25.06 nm and length is about 23.58 nm. Also it showed smooth surfaces of the particles and mostly non-agglomerated (Fig. 2).

The XRD pattern of the prepared NZBG is represented in Fig. 3. The XRD pattern, reveals an amorphous nature and there is no detectable peaks in the pattern. This indicated that the prepared sample had an amorphous structure.

3.2 Fourier Transform Infrared Spectroscopy (FT-IR) of NZBG Bioactive Glass Powder

FTIR spectrum of NZBG is represented in Fig. 4. Silicate absorption bands assigned to peaks 1085, 900 and 464 Cm-1 respectively [21]. There are bands at 580 and 600 Cm-1which are illustrating a P-O bending oscillationdue to the existence of phosphate group [22].

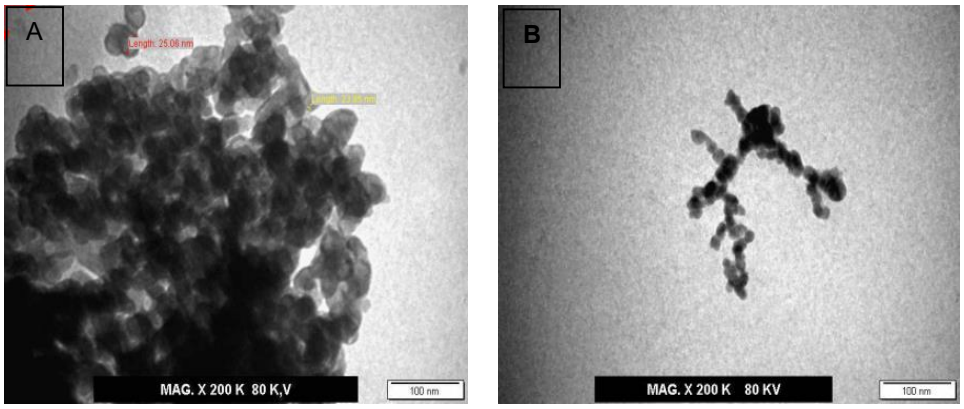

Fig. 2. TEM showing the nano particles' diameter is 25.06 nm and length is about 23.58 nm (A&B)

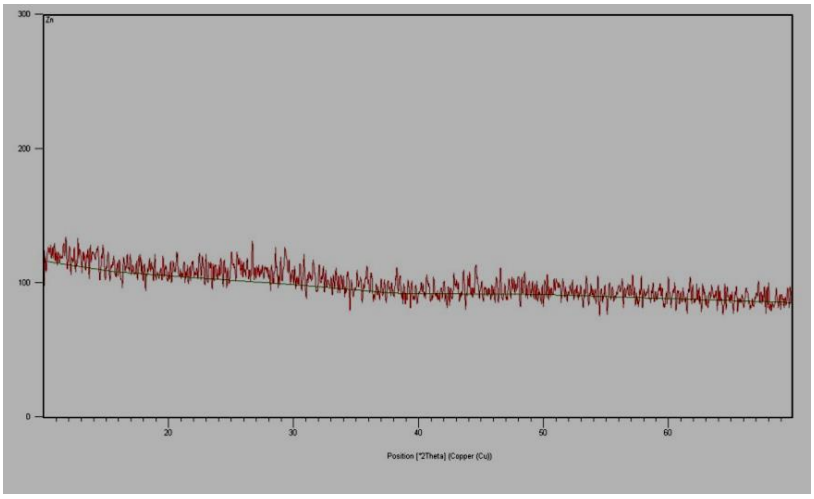

Fig. 3. XRD pattern of the prepared NZBG bioactive glass powder

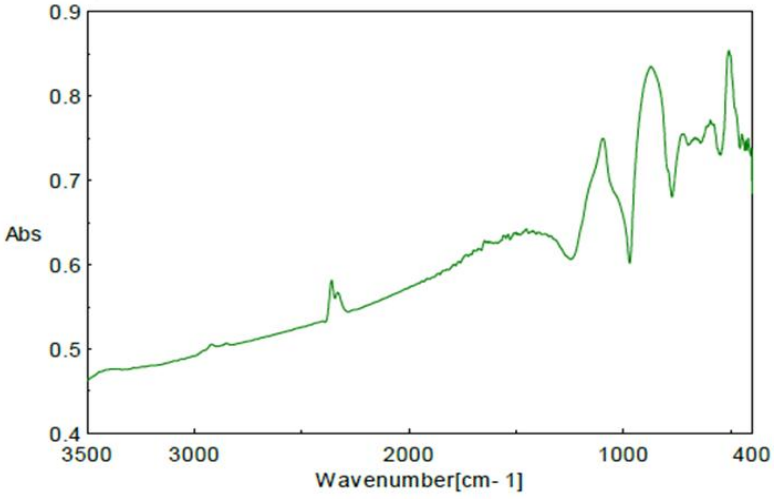

Fig. 4. FTIR of the prepared NZBG bioactive glass powder

3.3 Microscopic Examination of 2nd Trimester AF-derived MSCs of Sample at Different Passages

Showed the morphology of the primary aggregate of human 2nd-trimester derived stem cells (AFSCs) with its cuboidal morphology Fig. 5 (A). 2nd trimester AF-derived MSCs of sample showed highly proliferative typical MSCs morphology at subsequent passages Fig. 5 (B).

3.4 Alizarin red staining

Control plate, cultured of AF-MSCs in regular proliferation media showed no Alizarin Red staining (Fig 6. A), while AF-MSCs culture in osteogenic media were stained by Alizarin Red staining for detection of orange-red calcium spots after 21 of the osteogenic induction showed staining for Alizarin Red staining of calcium nodules in all the parts of the plate (Fig. 6.B).

3.5 Scanning Electron Microscopy (SEM) of Osteogenic Stem Cells on Nano-Bioactive Glass Disks

SEM observation of the cultured cells showed that proliferation of AFSC was accompanied by the production of clusters of bone like apatite mineralization in multilayer arrangements surrounded by extracellular fibers (Figs. 7, 8).

These mineral globules shown by X-ray microanalysis to contain Ca and P (Fig. 9). The scaffold was wrapped with osteoblasts and the cells were ribbed in shape. In some osteoblasts,

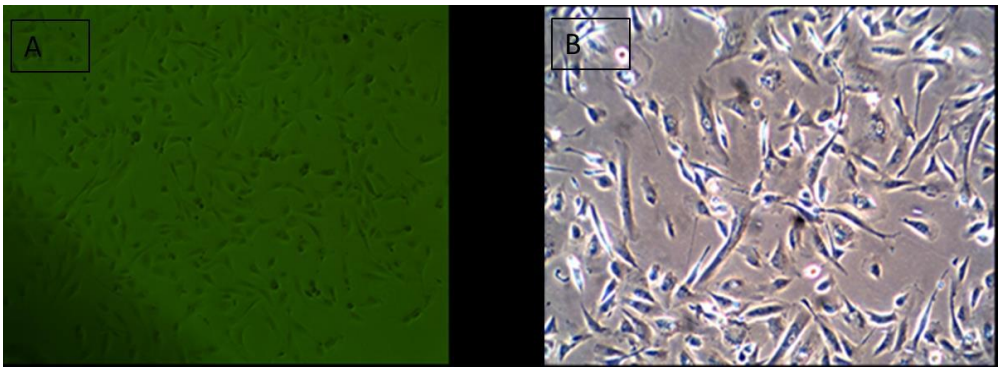

Fig. 5. Follow up of progression of 2nd trimester AF- MSCs of sample at different passages: AF-MSCs at (A): P0, day 7 and (B): P2 at day 3. (A) Showed the morphology of the primary aggregate of human 2nd-trimester derived stem cells (AFSCs) with its cuboidal morphology, (B) showed the highly proliferative typical MSCs morphology

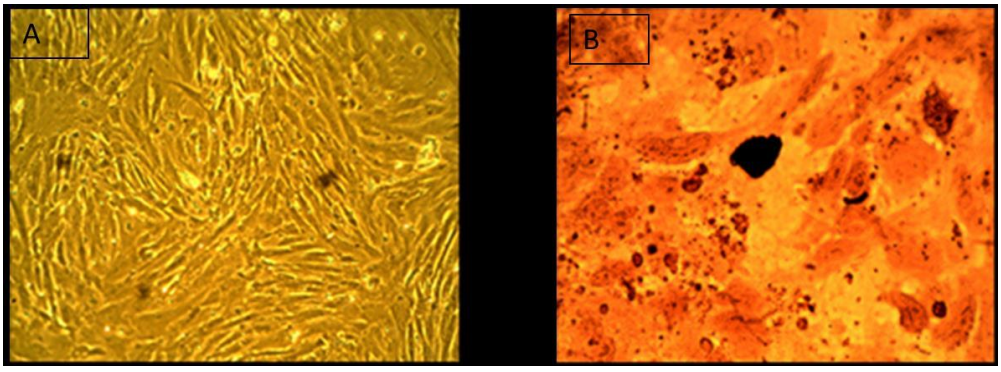

Fig. 6. Osteogenic differentiation potential of AF-MSCs cultured in MSCs proliferation media and AF-MSCs in osteogenic media. AF-MSCs stained by Alizarin Red stain for detection of orange-red calcium spots, on day, 21 of the osteogenic induction. (A) Control plate showed no staining for Alizarin. (B) Osteogenic plate showed multiple stained spots in different parts of the plate

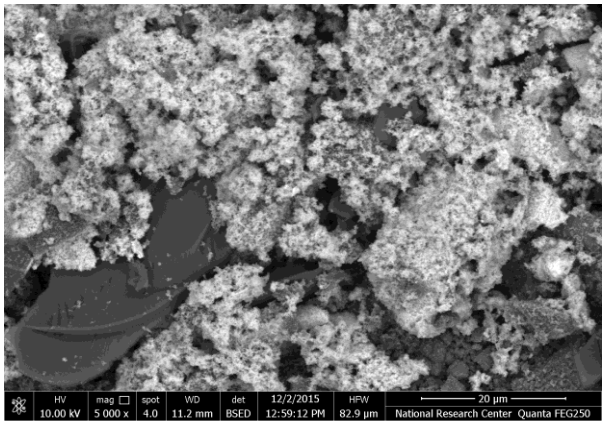

Fig. 7. SEM of the prepared NZBG bioactive glass disk with osteogenic cells for one week

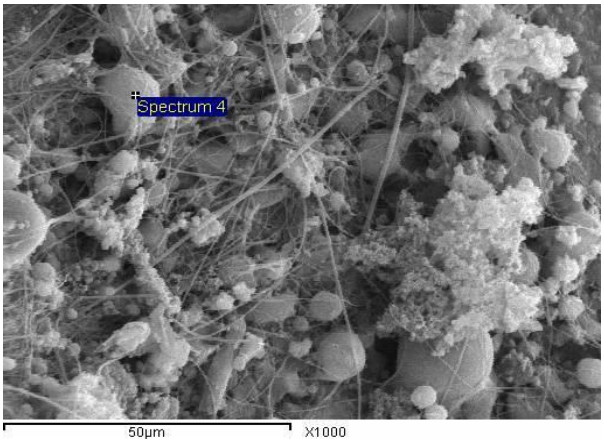

Fig. 8. The scffold completely covered with osteoblast of polygonal shape (C) and many mineral golobules observed (M). Extracellular fibers of huge amount reflecting the secretory activity of the cells

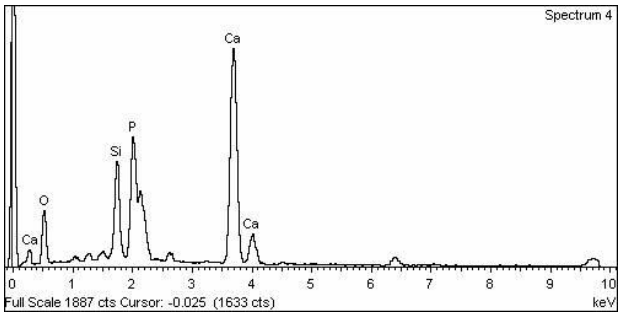

Fig. 9. The mineral globules shown by X-ray microanalysis (EDAX) to contain Ca and P

many teeny junction cohesions had expanded from the cells in the scaffolds, and the cells were collected with more closely and were incorporated, denoting that osteoblasts were increased their secretion. These results indicting the osteogenic functions and rapid bone formation of novel bioactive glass after incubation with human osteogenic cells in-vitro was beginning 7 days. The typical overview of osteogenic cells morphologies after incubated 21 days.

3.6 Histological Results

3.6.1 At first week

The biopsies harvested from the defects of group A1 were filled with granulation tissue containing large number of large-sized blood sinusoids (Fig. 10A,B). The newly formed bone at the defect borders was formed of immature bone trabeculae containing large number of osteocytes, large number of marrow spaces. Bone trabeculae began to invade the fibrous tissue formed on top of the granulation tissue. Many chronic inflammatory cells appeared within the granulation tissue. In group B1 (Fig. 10C & D) the new bone began to invade the fibrous tissue surrounding the granulation tissue. The defects were partially filled by bone trabeculae with intervening interconnected marrow spaces network. No evidence of chronic inflammatory cell infiltrates.

3.6.2 At second week

In group A2 the defects were partially filled by thicker bone trabeculae with large intervening interconnected marrow spaces network (Fig. 11A, B). While group B2, at the fundus of the defects, bone trabeculae were formed to close the holes. The defects were partially closed from their borders with lacerated bone trabeculae containing large number of osteocytes and intervening marrow spaces (Fig. 11C, D).

3.6.3 At third week

The defect in group A3 closed with bridges of interconnected homogenous bone trabeculae with large marrow spaces and large number of osteocytes. The bone center was filled with fatty bone marrow and surrounded with less granulation tissue (Fig. 12 A, B). The defects in group B3 were completely closed with lamellar bone with regular Haversian systems. The arrangement of bone was more mature with numerous osteons and few entrapped osteocytes (Fig. 12C, D).

3.7 Statistical Results

The comparative analysis regarding Area % between the studied groups was recorded in Table 3. Statistical significant difference was noticed between the six groups, according to ANOVA test.

On the other hand, 2-groups comparison (Post-hoc test) of the mean values ± SD as regard new bone formation results at the first, second & third week post-operative in the control and experimental groups showed a statistically highly significant difference between each pair of the studied groups as the p-value was < 0.01.

Table 3. Statistical significant difference

Groups	Number	Mean ± STD
Group 1A	10	19.765±6.087*
Group 1B	10	42.99±3.44*
Group 2 A	10	35.23±0.33*
Group 2 B	10	75.84±1.33*
Group 3 A	10	51.34±0.12*
Group 3 B	10	95.56±0.35*

*ANOVA = 62.8 *P value < 0.001 (very highly significant)*

4. DISCUSSION

The current study was conducted to evaluate the biocompatibility and osteogenic potential of the prepared novel nano-bioactive glass including zirconium (NZBG). The results of PCS and Transmission electron microscopic examination (TEM) of the powder morphology showed that the product is composed of nanostructures. The diameter is 25.06 nm and length is about 23.58 nm. Also it showed smooth

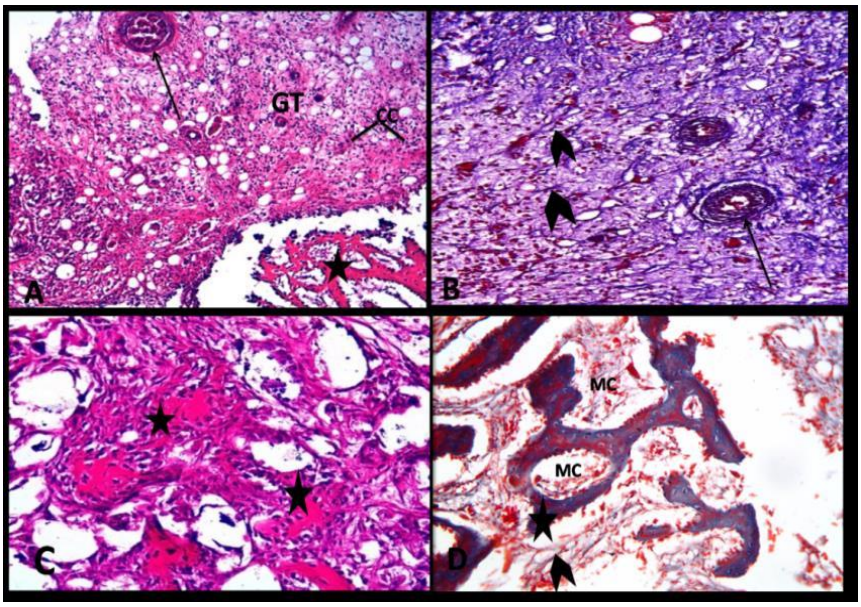

Fig. 10. A photomicrograph of group A1 (A& B) showing, the granulation tissue (GT) containing chronic inflammatory cell infiltrates (CC), few interconnected newly formed bone trabeculae (astrickes), immature collagen fibers (arrow heads) and large number of large-sized blood sinusoids (arrow). Group B1 (C &D) showing, bone trabeculae (asterisks), immature collagen fibers (arrow heads) & interconnected marrow cavities (MC). (A & C) (H&E stain, Orig. Mag. 200x,); (B& D) (Masson Trichrom stain, Orig. Mag. 200x)

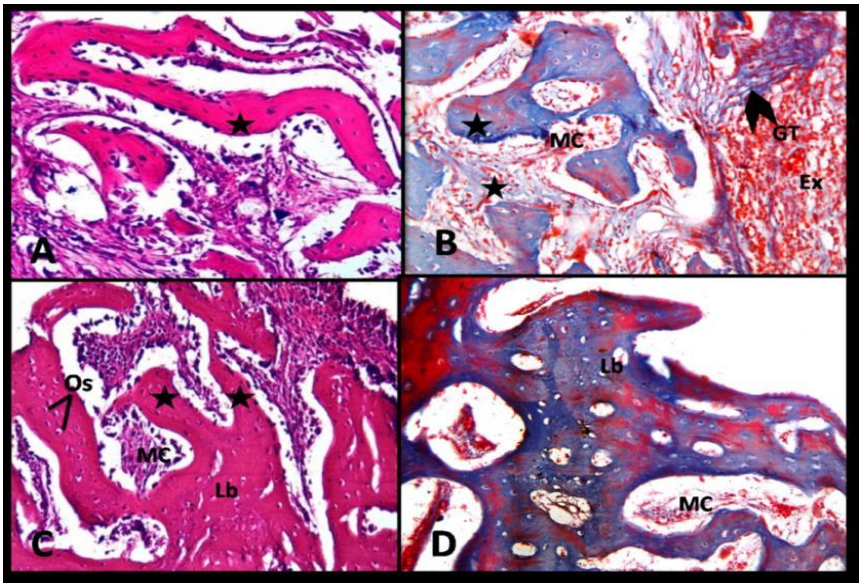

Fig. 11. A photomicrograph of group A2 (A& B) showing, the granulation tissue (GT) with extravasated RBCs (Ex), new bone trabeculae (asterisks), immature collagen fibers (arrow heads)& interconnected marrow cavities (MC). Group B2 (C &D) showing, thicker bone trabeculae (asterisks), interconnected marrow cavities (MC), many osteocytes (Os) and lamellar bone (Lb). (A & C) (H&E stain, Orig. Mag. 200x,); (B& D) (Masson Trichrom stain, Orig. Mag. 200x)

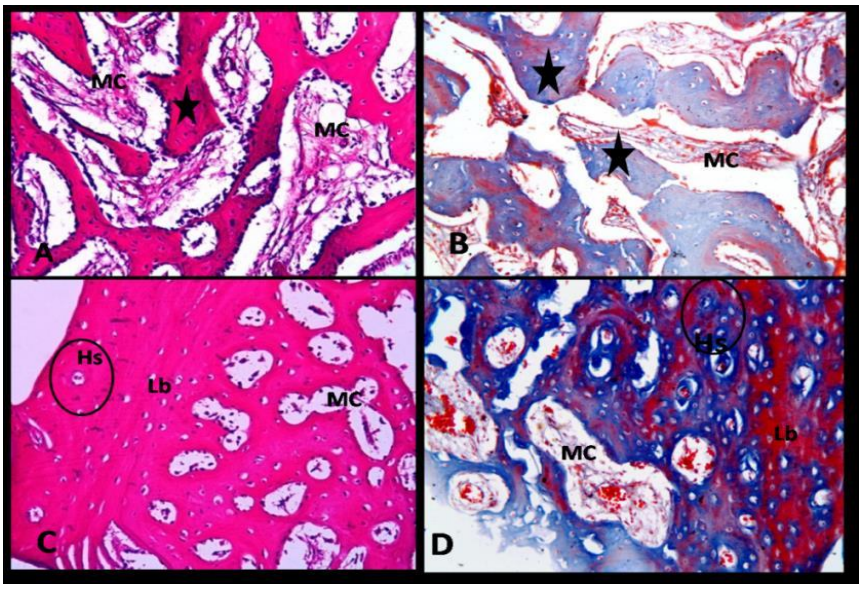

Fig. 12. A photomicrograph of group A3 (A& B) showing, the defect closed with bridges of interconnected bone trabeculae (asterisk) with large marrow spaces (Mc). Group B2 (C &D) showing, the defects were completely closed with more mature lamellar bone (Lb) and Haversian systems (Hs). (A & C) (H&E stain, Orig. Mag. 200x,); (B& D) (Masson Trichrom stain, Orig. Mag. 200x)

surfaces of the particles and mostly non-agglomerated. Also the XRD proved amorphous nature of the NZBG. In this investigation amniotic fluid samples, directly cultured in

osteogenic medium were able to produce osteogenic cells as demonstrated by Alizarin Red staining that was agreed with Antonucci et al., 2009. Several embryonic stem cells, AFMSCs are not tumorigenic (forming cancer cells) and can extend without the use of intensive layers or costly defined media [14].

SEM of NZBG disks cultured with AF- MSCs proved the production of clusters of bone like apatite mineralization in multilayer arrangements surrounded by extracellular fibers. In vitro investigations have determined that bioactive glass spurred osteoprogenitor to differentiate to mature osteoblasts that output bone-like apatite nodules [23,24]. It has been agreeable that the bioactive characteristic of the scaffold biomaterials is their ability to bond with living bone through the e formation of a bone –like apatite layer on their surface both in vitro and in vivo. In this work, FTIR spectra and SEM evaluated and proved the bone like apatite-mineralization capability of the NZBG scaffolds. It is interesting that the Zr incorporation in the BG NZBG glass significantly reinforced AF-MSCs attachment and proliferation. The bonding between cells and biomaterials is obtained by many factors, such as increased secretory activity of the differentiated osteoblasts forming the extracellular fibers [25].

In vivo investigation of NZBG scaffold was evaluated histologically, histochemically and histomorphometrically. Histological results disclosed that the implantation of Zr enriched bioactive glass has obviously accelerated the bone healing by enhancing the rate of the newly formed bone trabeculae and decreasing the chronic inflammatory cell infiltrates. The bioactive glass (BG) is utilized in a variety of dental proceedings [26], and numerous bioactive glass compositions can be generated into scaffolds for tissue engineering [27]. The bioactive glass (BG) has surface reactivity and BG also liberation ions that promote the osteoblast phenotype [28,29].

Moreover, nanotechnology prolonged new nano-materials to improve the strength and toughness of bioactive ceramics. Bioactive nano-glasses show magnificent potential for bone repair as compared with conventional ones due to best mechanical and biological properties [30]. Hydroxyapatite (HA) as bioactive glass is utilized extensively in biomedical purposes to replacement the bone tissues [31,32]. Dentistry and orthopaedic applications agree that the hydroxyapatite has a good biocompatibility, osteoconductivity and the bone-bonding properties [33].

Zirconia is ceramic filler among many fillers or reinforcements, which has been used to increase the strength and toughness of many bioactive glass materials [32]. Zirconia has shown very wide applications in bone surgery [34]. The result of this study proved that in zirconium ions there was less chronic inflammatory cell infiltrates which could be explained on the bases of the hydroxyapatite zirconia has smoother surface than hydroxyapatite [34]. Bacteria coherence to a biomaterial surface deepened on the surface roughness or physical configuration of the material [35]. So there was less numbers of bacterial invasion and so less inflammation.

Moreover, it is obtained that the zirconia particles added in the pores among the particles of hydroxyapatite. It can be understood that hydroxyapatite-zirconia has less porous structure compared to hydroxyapatite without zirconia. Material without pores among particles gives smoother surface of the material [36]. Also the results in the present study were in agreed other study concluded that adding (5) wt. % of (ZrO_2) helps and accelerates the healing process of the bone [37]. Histological observations confirmed the post-operative clinical evaluation of the animals. There were no negative signs such as suppuration, pain or weight loss. It is worth noting that although the defects in the rabbits' tibia were not of critical size; they were fully repaired with bone in direct contact with the biomaterials, confirming their biocompatibility and osteoconductivity.

5. CONCLUSION

Our work has led us to conclude that, the culture of AF-stem cells with NZBG bioactive glass disks were enhanced osteoblastic proliferation and clusters of bone like apatite mineralization in multilayer arrangements that increased by time in-vitro experiments. While the in-vivo, histopathology and electron microscope results demonstrated a well healing of the defect filled with NZBG bioactive glass regarding the bone quality and quantity in comparison to the control group.an enhanced biocompatibility and faster osteogenesis with prepared NZBG bioactive glass. The results of this study achieved a good potential application for the bone regeneration medicine.

ETHICAL APPROVAL

All authors have obtained all necessary ethical approval from National research Center Committee.

All authors hereby declare that "Principles of laboratory animal care" (NIH publication No. 85-23, revised 1985) were followed, as well as specific national laws where applicable. All experiments have been examined and approved by National Research Center committee.

All authors hereby declare that all experiments have been examined and approved by National Research Center committee and have therefore been performed in accordance with the ethical standards laid down in the 1964 Declaration of Helsinki.

ACKNOWLEDGEMENTS

We would like to express our great thanks and appreciation to Dr. Alice K. Abdel Aleem, Professor of Human Genetics, Molecular Medical Genetics department/ Head of Stem Cell Research Group, for her initiation and established of Stem Cell Research in Center of Excellency for Advanced Science (CEAS), National Research Centre.

COMPETING INTERESTS

Authors have declared that no competing interests exist.

REFERENCES

1. Hench Ll. The story of bioglass. J Mater Sci Mater Med. 2006;17(11):967-978.
2. Liu C, Xia Z, JT C. Design and development of three-dimensional scaffolds for tissue engineering. Chemical Engineering Research and Design. 2007; 85(7):1051-1064.
3. Mônica Diuana Calasans-Maia, Fabio Oliveira Ascoli, Adriana Terezinha Neves Alves Novellino, Alexandre Malta Rossi, Granjeiroi. Jm. Comparative histological evaluation of tibil bone repair in rabbits treated with xenografts. Acta Ortop Bras. 2009;17(6).
4. Kimelman N, Pelled G, Helm Ga, Huard J, Schwarz Em, Gazit D. Review: Gene- and stem cell-based therapeutics for bone regeneration and repair. Tissue Eng. 2007;13(6):1135-1150.
5. Eid K, Zelicof S, Perona Bp, Sledge Cb, Glowacki J. Tissue reactions to particles of bone-substitute materials in intraosseous and heterotopic sites in rats: discrimination of osteoinduction, osteocompatibility, and inflammation. J Orthop Res. 2001;19(5):962-969.
6. Kokubo T. Bioactive glass ceramics: Properties and applications. Biomaterials. 1991;12(2):155-163.
7. Legeros Rz. Properties of osteoconductive biomaterials: Calcium phosphates. Clin Orthop Relat Res. 2002;395:81-98.
8. Hench LL, Splinter RJ, Allen WC, K. Gt. Bonding mechanisms at the interface of ceramic prosthetic materials. Biomedical Materials Research. 1971;2(1):117-141.
9. Jones Jr. Review of bioactive glass: From hench to hybrids. Acta Biomater. 2013; 9(1):4457-4486.
10. Ahmad A, Ziauddin A, A. Rs. Solation and culture of human amniotic fluid stem cells (Afscs). Pak J Health Research. 2013; 1(1):32-35.
11. Maraldi T, Riccio M, Resca E, Pisciotta A, La Sala Gb, Ferrari A, Bruzzesi G, Motta A, Migliaresi C, Marzona L et al. Human amniotic fluid stem cells seeded in fibroin scaffold produce *in vivo* mineralized matrix. Tissue Eng Part A. 2011,17(21-22):2833-2843.
12. Maziar Montazeriana, José Fabián Schneiderb, Bijan Eftekhari Yektaa, Vahak Kaspari Marghussiana, Alisson Mendes Rodriguesc, Zanottoc. Ed. Sol–gel synthesis, structure, sintering and properties of bioactive and inert nano-apatite–zirconia glass– ceramics. Ceramics International. 2015;41(9):11024-11045.
13. Antonucci I, Iezzi I, Morizio E, Mastrangelo F, Pantalone A, Mattioli-Belmonte M, Gigante A, Salini V, Calabrese G, Tete S, et al. Isolation of osteogenic progenitors from human amniotic fluid using a single step culture protocol. Bmc Biotechnol. 2009;9:9.
14. De Coppi P, Bartsch G, Jr, Siddiqui Mm, Xu T, Santos Cc, Perin L, Mostoslavsky G, Serre Ac, Snyder Ey, Yoo Jj et al. Isolation of amniotic stem cell lines with potential for therapy. Nat Biotechnol. 2007; 25(1):100-106.

15. Zhang S, Geng H, Xie H, Wu Q, Ma X, Zhou J, Chen F. The heterogeneity of cell subtypes from a primary culture of human amniotic fluid. Cell Mol Biol Lett. 2010;15(3):424-439.
16. Gregory Ca, Gunn Wg, Peister A, Prockop Dj. An alizarin red-based assay of mineralization by adherent cells in culture: Comparison with cetylpyridinium chloride extraction. Anal Biochem. 2004; 329(1):77-84.
17. Ioannis Papantoniou, Maarten Sonnaert, Toon Lambrechts, Jean-Marie Aerts, Lies Geris, Frank P. Luyten, Schrooten. J. Analysis of gene expression signatures for osteogenic 3d perfusion-bioreactor cell cultures based on a multifactorial doe approach. Processes. 2014;2(3):639-657.
18. Zavatti M, Bertoni L, Maraldi T, Resca E, Beretti F, Guida M, La Sala Gb, De Pol A. Critical-size bone defect repair using amniotic fluid stem cell/collagen constructs: Effect of oral ferutinin treatment in rats. Life Sci. 2015;121:174-183.
19. Patrick JM, Danel HR, ENC. The biology of the laboratory rabbit. Academic Press, New York. 1994;468-468.
20. Parfitt Am, Drezner Mk, Glorieux Fh, Kanis Ja, Malluche H, Meunier Pj, Ott Sm, Recker Rr. Bone histomorphometry: Standardization of nomenclature, symbols, and units. Report of the Asbmr Histomorphometry Nomenclature Committee. J Bone Miner Res. 1987; 2(6):595-610.
21. Erol-Taygun M, Zheng K, ARB. Nano-scale bioactive glass in medical application. Intjappglass Sci. 2013; 4(2):136–148.
22. MM. Effect of Zro2 addition on properties of gel-derived bioactive Sio2–Cao–P2o5 glass–ceramics. Iran University of Science And Technology; 2015.
23. Tsigkou O, Hench Ll, Boccaccini Ar, Polak Jm, Stevens Mm. Enhanced differentiation and mineralization of human fetal osteoblasts on pdlla containing bioglass composite films in the absence of osteogenic supplements. J Biomed Mater Res A. 2007;80(4):837-851.
24. Tsigkou O, Jones Jr, Polak Jm, Stevens Mm. Differentiation of fetal osteoblasts and formation of mineralized bone nodules by 45s5 bioglass conditioned medium in the absence of osteogenic supplements. Biomaterials. 2009; 30(21):3542-3550.
25. Yufang Zhu, Yufeng Zhang, Chengtie Wu, Ying Fang, Junhe Yang, Wang S. The effect of zirconium incorporation on the physiochemical and biological properties of mesoporous bioactive glasses scaffolds. Microporous and Mesoporous Materials. 2011;143(2-3):311-319.
26. Shapoff Ca, Alexander Dc, Clark Ae. Clinical use of a bioactive glass particulate in the treatment of human osseous defects. Compend Contin Educ Dent. 1997; 18(4):352-354,356,358 Passim.
27. Jones JR, Gentleman E, Polakj. Bioactive glass scaffolds for bone regeneration. Elements. 2007;3(3):393-399.
28. Effah Kaufmann Ea, Ducheyne P, Shapiro Im. Evaluation of osteoblast response to porous bioactive glass (45s5) substrates by Rt-Pcr analysis. Tissue Eng. 2000; 6(1):19-28.
29. Jell G, Notingher I, Tsigkou O, Notingher P, Polak Jm, Hench Ll, Stevens Mm. Bioactive glass-induced osteoblast differentiation: A noninvasive spectroscopic study. J Biomed Mater Res A. 2008;86(1):31-40.
30. Du Rl, Chang J, Ni Sy, Zhai Wy, Wang Jy. Characterization and in vitro bioactivity of zinc-containing bioactive glass and glass-ceramics. J Biomater Appl. 2006; 20(4):341-360.
31. Wang Q, Ge S, DZ. Highly bioactive nano-hydroxyapatite partially stabilized zirconia ceramics. Journal of Bionics Engineering. 2004;1(4):215-220.
32. Nayak Y, Rana Rp, Pratihar Sk, Bhattacharyya S. Pressureless sintering of dense hydroxyapatite-zirconia composites. J Mater Sci Mater Med. 2008;19(6):2437-2444.
33. Simon CG, Antonucci JM, Liu DW, DS. *In vitro* cytotoxicity of amorphous calcium phosphate composites. *J Bioact Compat Polym.* 2005;20(3):279-295.
34. Quan R, Yang D, Wu X, Wang H, Miao X, Li W. *In vitro* and *in vivo* biocompatibility of graded hydroxyapatite-zirconia composite bioceramic. J Mater Sci Mater Med. 2008; 19(1):183-187.
35. Katsikogianni M, Missirlis Yf. Concise review of mechanisms of bacterial

adhesion to biomaterials and of techniques used in estimating bacteria-material interactions. Eur Cell Mater. 2004;8:37-57.

36. Ahn ES, Gleason NJ, Y Yj. The effect of zirconia reinforcing agents on the microstructure and mechanical properties of hydroxyapatite-based nanocomposites. Journal of the American Ceramic Society. 2005;88(12):3374-3379.

37. Waleed A. Hanna, Sahib Al-Saffar, Hassan B. The effect of 5 Wt %yettria- stabilized zirconia on crystallized glass-ceramic system at different temperature Jkau. Eng Sci. 2011;22(1):3-16.

Peer-review history:
The peer review history for this paper can be accessed here:
http://sciencedomain.org/review-history/21998